Entrained-flow gasification of torrefied tomato peels: combining torrefaction experiments with chemical equilibrium modeling for gasification

Paola Brachi[a1], Riccardo Chirone[a], Francesco Miccio[b], Michele Miccio[c], Giovanna Ruoppolo[b]

[a]*Institute for Research on Combustion (IRC-CNR), P.le Tecchio 80, 80125 Napoli, Italy*

[b]*Institute of Science and Technology for Ceramics (ISTEC-CNR), via Granarolo 64, 48018 Faenza (RA), Italy*

[c]*Department of Industrial Engineering, University of Salerno, via Giovanni Paolo II 132, 84084 Fisciano (SA), Italy*

Abstract

The purpose of the present study is to quantify the impact of torrefaction pretreatment on the quality of the product gas arising from the gasification with steam and steam-oxygen mixtures of non-woody biomass in high-temperature entrained flow reactors. To this aim, a chemical equilibrium model for biomass gasification was developed, which allowed predicting the product gas composition as a function of process temperature, equivalence ratio, steam-to-biomass ratio and biomass elemental composition. A global sensitivity analysis with respect to the model input parameters was performed to assess the impact of torrefaction and gasification operating conditions on the quality of the product gas in terms of heating value and composition metrics typically adopted in the process industry (H_2/CO ratio, stoichiometric module, etc.). In particular, the gasification of raw tomato peels and consequent torrefied solids resulting from fluidized bed batch torrefaction tests performed under light (200 °C and 30 min), medium (240 °C and 30 min) and severe (285 °C and 30 min) conditions was investigated using ultimate analysis data in the model. Results of this analysis highlighted that the quality of product gas arising from the oxygen-steam gasification of torrefied and untreated tomato peels did not differ very much, although torrefied

[1] Corresponding author. Tel.: +39 081 7682245.
E-mail address: p.brachi@irc.cnr.it

feedstocks produced more H_2 and CO and less CO_2 than the parent one. This suggests that, despite the significant benefits it determines in biomass feeding, grinding and storage, the torrefaction pretreatment provides only a marginal improvement in the product gas quality. Equilibrium simulations made available in the present study can be useful for a better understanding of the controlling variables that rule gasification processes in addition to act as a point of reference for more complex simulations of the high temperature entrained flow gasification of biomass with oxygen-steam mixtures.

Keywords: Agro-industrial residues; Fluidized bed Torrefaction; Entrained Flow Gasification; Equilibrium modeling; Tomato peels; Oxygen-steam gasification.

1. Introduction

Biomass is an abundant, renewable, and environmentally carbon-neutral energy resource. Its exploitation can contribute to reducing both the dependence on fossil fuels and the net CO_2 emissions. A considerable amount of research papers published in pertinent areas [1-3] describe gasification as the most promising thermochemical pathway for the above purpose due to its flexibility to convert any type of biomass, including agricultural residues, non-fermentable byproducts from biorefineries, byproducts of food industry and even organic municipal wastes, into a variety of fuels and chemicals in addition to energy [4]. Moreover, as regard heat and power generation, applied research also shows that for a given energy throughput, the amount of major air pollutants (i.e., CO_2, NO_x, SO_2, particulates) arising from an integrated gasification combined cycle (IGCC) power plant are lower than those from direct combustion systems [5].

Gasification is the conversion by partial oxidation of a carbonaceous feedstock (e.g., biomass or coal) into a gaseous energy carrier, known as "producer gas", which contains hydrogen (H_2), carbon monoxide (CO), carbon dioxide (CO_2), methane (CH_4), water (H_2O), nitrogen (if air is used as the oxidizing agent), trace amounts of light hydrocarbons and various contaminants such as

small unconverted char particles, ash and tars (i.e., a complex mixture of different condensable hydrocarbons). It takes place at temperatures between 600 and 1400 °C and at a pressure in the range of 1-33 bar [6]. The partial oxidation can be carried out using air, oxygen, steam or a mixture of these as a gasifying agent. Air gasification typically produces a low heating value gas (4-7 MJ/Nm^3 higher heating value [7]) suitable for boiler, turbine and engine operation but not for pipeline transportation due to its low energy density arising from nitrogen dilution. Oxygen gasification produces a high to medium calorific value gas (12-28 MJ/Nm^3 higher heating value [7]) suitable for limited pipeline distribution and as synthesis gas for conversion into a variety of fuels (H_2, Fischer-Tropsch diesels and synthetic gasoline) and chemicals (methanol, urea), even though the high capital cost for oxygen production is the main barrier to its use. Steam is another possible gasifying agent that can yield a medium heating value (10-16 MJ/Nm^3, [7]) gas. However, the process would become more sophisticate, as indirect or external heating is needed for the endothermic reactions [3]. At present, gasification with air is the more widely used technology since there are neither the cost nor hazard of oxygen production and usage, nor the complexity and cost of multiple reactors. Steam-oxygen [3, 4, 8] and steam-oxygen enriched air [9] gasification processes have also been studied to some extent due to their many different applications. Various types of reactors have been explored for biomass gasification so far, which include fixed-bed gasifiers, operated in counter-current, co-current [8] or cross-current mode [10], fluidized bed gasifiers [4] and entrained flow gasifiers [11]. Compared with fixed-bed and fluidized bed gasification, entrained flow gasification operates at higher temperatures (> 1200 °C) and with smaller particles (< 500 μm) allowing to achieve a higher carbon conversion and to produce a high quality syngas with negligible methane and tar content [12]. However, the size reduction of biomass, typically required in entrained-flow systems, may be expensive and very difficult to achieve for some biomass feedstocks due to the inherent fibrous structure and very low grindability [13]. Accordingly, a lower number of experimental studies has been published so far on biomass gasification in entrained flow reactors compared to those concerning fossil fuels. These studies were performed at both relatively

low (900-1100 °C) and high (1200-1400 °C) temperatures and investigated mostly the effects of the reaction temperature, the excess air ratio, the water addition and the biomass type on the distribution and the composition of solid (soot and char), liquid (tar) and gas products [14-16]. The influence of the particle size and residence time on the gasifier performance and the producer gas quality [17] as well as the impact of the catalytic activity of alkali metal species on the formation of soot, tar and char [18] have also received some attention. In more details, experiments by Hernández et al. [15] showed that that an increase in the operating temperature can have different effects depending on the gasifying agent used. For example, air gasification mainly increases the CO and H_2 concentration in the product gas via the endothermic Boudouard and steam reforming reactions, whereas gasification processes with air–steam leads to a boost in the H_2 production due to the enhancement of the char-steam reforming and WGS (water–gas shift) reactions, as well as an increase in the CH_4 content. Again, investigations by Qin et al. [16] showed that the carbon conversion during biomass gasification is higher than 90 %wt. at the optimal conditions of 1400 °C with steam addition and that the syngas contained nearly no tar. In addition, they also found that, during the entrained flow gasification processes, the carbon in biomass not converted to gas only appeared as soot particles, except for experiments performed at lower temperatures (around 1000 °C), where a very small amount of char was also left. To enable and facilitate the biomass gasification in entrained-flow reactors, a variety of pretreatment methods for improving the properties of raw biomass have been developed, including hydrothermal carbonization [19], pyrolysis [20] and torrefaction [21, 22]; among them torrefaction seems to be the most promising one [13].

Torrefaction is a mild thermal treatment where raw biomass is heated in an inert environment to a temperature ranging between 200 and 300 °C. It is traditionally characterized by low particle heating rate (typically less than 50 °C/min) and by a relatively long reactor residence time that ranges from 15 to 120 minutes depending on the specific feedstock, technology and temperature. After torrefaction, the fuel properties of biomass are deeply improved [23, 24]. In

particular, torrefied solids have lower moisture content, higher hydrophobicity, intensified energy density and improved storability in comparison to their parent feedstocks. Moreover, the fibrous structure of fresh biomass is partially destroyed by torrefaction thus making easier its size reduction. Finally, pulverized particles obtained from torrefied biomass are more spherical and this makes them more easily fluidizable or flowable [25] and less prone to agglomeration in pneumatic dense flow feeding systems [23, 26]. Due to these benefits, there has been much interest in torrefaction and several studies have been done to understand this process [13, 24, 27]. However, the application of torrefied biomass in gasification remains largely unexplored. To the best of our knowledge, no works can be found in literature on the impact of torrefaction on the behavior of non-woody biomass (e.g., low-value agro-industrial residues) during gasification with steam and oxygen at high temperature in an entrained flow reactor, in terms of neither syngas quality nor solid gasification kinetics. Therefore, a systematic study on torrefied non-woody biomass gasification in entrained flow reactor is of great practical and scientific interest.

As a continuation of a previous study aimed at assessing the potential of fluidized bed torrefaction treatment in improving the fuel properties of low value agro-industrial residues (i.e., tomato peels) [24], the idea behind this work was that of considering the addition of a torrefaction stage prior to gasification. Therefore, the first objective of the present paper was to investigate the influence of torrefaction on the quality of the product gas arising from the oxygen-steam gasification in high temperature entrained flow reactors; the second one was to determine operating conditions beneficial for obtaining a product gas suitable for synthesis or, alternatively, heat and power production. To this aim, a chemical equilibrium model for biomass gasification was developed, which allowed the prediction of the syngas composition as a function of the gasification temperature (T), the fuel-oxygen equivalence ratio (ER), the steam-to-biomass ratio (SBR) and the elemental composition of the biomass. A global sensitivity analysis with respect to the model input parameters was performed to assess the impact of both the torrefaction pretreatment and the gasification operating conditions on the product gas quality in terms of heating value and

composition metrics typically adopted in process industry (i.e., H_2/CO ratio, stoichiometric module M, etc.).

2. Material and methods

2.1 Feedstock properties and operating conditions

Tomato peels, which are the residues of peeling tomato used for canning [28], were used as biomass feedstock for this research work as they represent a widespread agro-industrial residue in the Campania region of Italy, with good potential for energy application [24]. Torrefaction tests, which for sake of brevity will not described in detail, were performed in a batch lab-scale fluidized bed reactor. The experimental runs were performed at 200, 240 and 285 °C and for holding times equal to 5, 15 and 30 min. Specific details about the test facility and the adopted experimental procedures are described in a previous work by the present authors [24]. Briefly, results showed that the torrefaction treatment of tomato peels led to a significant improvement in both their physical and chemical properties. More specifically, the calorific value increased by a factor of 1.2 for the biomass treated at 285 °C and 30 min. Under the same experimental conditions, a 40 % reduction in the O/C elemental ratio and an improved hydrophobicity of the torrefied tomato peels were also observed. These positive effects of the torrefaction treatment occurred while maintaining the mass yield (approximately between 75 and 94 %, daf) and energy yield (approximately 90 and 96 %, daf) at satisfactory levels [24].

The gasification process was simulated by using four selected biomass feedstocks, namely raw tomato peels (TPs) and tomato peels torrefied at 200 °C (TP-200), 240 °C (TP-240) and 285 °C (TP-285), with 30 min holding times in the adopted lab-scale fluidized bed reactor. The elemental composition and the calorific values of the investigated biomass samples are shown in Table 1. To exclude the effect of the difference in the moisture content of the investigated biomass feedstocks, the same value of 5 %wt. was taken for all the samples. It is worth noting that 5 %wt. moisture

158 content represents a plausible amount of water in biomass after the torrefaction pretreatment stage
159 [24].
160
161 **2.2 Mathematical model**
162 The model simulates the gasification process in high temperature entrained flow gasifiers
163 where an oxygen-steam mixture is used as gasifying agent. The model is based on chemical
164 equilibrium calculations, which are performed by applying the stoichiometric method. The biomass
165 feeding rate, its ash and moisture content and its elemental composition are input parameters for
166 mass balance in the model along with the fuel-oxygen equivalence ratio and the steam-to-biomass
167 ratio (SBR). The former is defined as the ratio between the molar flow rate of the oxygen actually
168 introduced into the reactor and the stoichiometric molar flow rate of the oxygen required for a
169 complete combustion, whilst the latter is defined as the mass flow rate of the steam fed to the
170 reactor divided by the fuel mass flow rate on a dry ash-free basis. The main assumptions of the
171 adopted model are as follows: 1. the biomass is composed of carbon (C), hydrogen (H), oxygen (O)
172 and nitrogen (N) element only in addition to ash; 2. the gasifier is considered isothermal; 3. all
173 reactions are at the chemical equilibrium; 4. the reacting system is at atmospheric pressure.; 5. all
174 gases are treated as ideal; 6. the fixed carbon in biomass is assumed to be completely gasified and,
175 therefore, the formation of char carbon is neglected; 7. tar is not taken into account in the simulation
176 due to the high operating temperature of entrained flow gasifiers leading to an almost tar-free
177 syngas; 8. ash in biomass is assumed to be inert, i.e. it does not participate in the chemical reactions;
178 9. N_2 is considered to be inert through the gasifier and no nitrogen compounds are generated; and,
179 finally, 10. the producer gas is assumed to consist only of H_2, CO, CO_2, H_2O, CH_4 and N_2. Not all
180 of these assumptions are rigorously correct; however, they provide a reasonable first approximation
181 of gasification process, which occurs in high temperature entrained flow reactors. In this regard, it is
182 wort noting that, due to the complexity of the phenomena occurring during a gasification process,
183 every model is only an approximation of the reality, describing selected aspects of the process. A

model cannot have absolute validity, but it should be valid for the purpose for which it is constructed [29]. For example, due to the simple mathematical formulation, the rather strict assumptions and the short time required for computation (in comparison to other approaches, especially computational fluid dynamics, CFD), equilibrium models, in particular, are useful in the preliminary analysis and optimization of gasification processes; results obtained through equilibrium calculations typically act as a point of reference for more complex simulations [30]. Equilibrium models, in fact, allow assessing the influence of different operating parameters (e.g., equivalence ratio, kind of gasification medium, steam injection, oxygen enrichment, etc.) on the producer gas composition for a wide range of fuel compositions. In practice, deviations from equilibrium predictions are common and related mostly to the overestimated char conversion and the non-simulated formation of tar and methane, especially for low-temperature processes [31]. Moreover, in an equilibrium model it is also assumed that the analyzed gases are considered to behave ideally. This assumption, in particular, is correct only in conditions of low pressure (near to atmospheric pressure), since the values of equilibrium constants calculated for ideal gases deviate significantly from the real ones. In this situation, the fugacity of each compound of the reacting mixture should be taken into account [30]. Moreover, equilibrium models are zero-dimensional (i.e., the geometry of the reactor is not necessary) and assume a uniform temperature across the whole reactor despite a slit drop or rise in the temperature over time and within the space of the reactor can results in considerable changes in the equilibrium constant values and, hence, in significant deviation in the concentration of the syngas components [30]. However, despite the abovementioned rather strict assumptions and simplifications, the applicability of equilibrium models to the gasification process has generally been established [32, 33]. In particular, these models proved to be especially reliable at the high temperatures that occur in entrained flow gasifiers [34] as well as in presence of catalysts [35] due to the resulting kinetics enhancement, which allows reaching a state close to the thermodynamic equilibrium even under the occurrence of a short residence time of the reactants in the gasifier, neglectable tar formation and very low amount

of residual char and soot [15, 16]. On the other hand, in other situations, where the restrictive hypotheses of equilibrium models are not properly satisfied, it is possible to increase the accuracy of model results thorough a calibration procedure relying on the use of the modified equilibrium constants defined as the actual equilibrium constants multiplied by the degree of approach to equilibrium [36].

The model is based on the following global steam-oxygen gasification reaction:

$$C_xH_yO_zN_w + aH_2O + bH_2O + cO_2 = \gamma_{H2}H_2 + \gamma_{CO}CO + \gamma_{H2O}H_2O + \gamma_{CO2}CO_2 + \gamma_{CH4}CH_4 + \gamma_{N2}N_2 \quad (1)$$

where x, y, z, and w are the molar fractions of carbon, hydrogen, oxygen, and nitrogen in the dry fuel, which were determined from the ultimate analyses data (Table 1), *a* the moles of H_2O (moisture) per mole of processed dry fuel, while *b* and *c* are the molar flow rates of steam and oxygen fed to the reactor per mole of processed dry fuel. On the right-hand side of Eq. (1), γi coefficients are the unknown moles of gaseous species leaving the gasifier (i.e., i = H_2, CO, H_2O, CO_2, CH_4 and N_2) for mole of processed biomass. To determine the equilibrium composition of the producer gas, six equations are required, which correspond to the number of stable chemical species assumed in the model. In line with the stoichiometric method, they were derived by using mass balance equations and equilibrium constant relationships. In particular, the number of independent reactions needed for formulating the equilibrium equations was determined by applying the Gibb's rule of stoichiometry, as described by Tassios [37]. In detail, in the present case study, where no solid carbon residues (e.g., soot or char) are assumed to remain in the gasification products, only two independent reactions needed to be considered in the equilibrium calculations.

Two common approaches are typically taken in the pertinent literature when selecting the above mentioned independent reactions, namely: i. the selection of water-gas reaction (Eq. 2) together with hydrogenating gasification (Eq. 3) as the main gasification reactions; and ii. the selection of water-gas shift reaction (Eq.4) along with the steam reforming of methane (Eq. 5) [38].

Water Gas Reaction	$C + H_2O \leftrightarrow CO + H_2$	(2)
Hydrogenating Gasification	$C+ 2H_2 \leftrightarrow CH_4$	(3)
Water Gas Shift	$CO+ H_2O \leftrightarrow CO_2 + H_2$	(4)
Methane Steam Reforming	$CH_4 + H_2O \leftrightarrow CO + 3H_2$	(5)

According to the theory of independent reactions, there is no significant difference between the above modeling approaches [37]. However, since the reactions involving steam are more favored in the case of steam gasification (high feed water content) [38, 39], the water gas shift (WGS) and the steam reforming of methane (MSR) were selected as independent reactions to be used in the present work. These reactions and, in particular, their equilibrium constants allowed generating two of the six equations required to determine the equilibrium composition of the produced syngas, as follows:

$$f1 = 0 = KWGS \cdot (\gamma_{CO}) \cdot (\gamma_{H2O}) - (\gamma_{CO2}) \cdot (\gamma_{H2}) \quad (6)$$

$$f2 = 0 = KMSR \cdot (\gamma_{CH4}) \cdot (\gamma_{H2O}) \cdot (\gamma_{total})^2 - (\gamma_{H2})^3 \cdot (\gamma_{CO}) \quad (7)$$

where KWGS and KMSR are the equilibrium constants for the water-gas shift reaction and the steam reforming reaction, respectively and γ_{total} is the molar flow rate of the producer gas. The remaining four equations were then derived by balancing the chemical elements involved in the global steam-oxygen gasification reaction in Eq.(1), as follows:

Carbon Balance:	$f3 = 0 = \gamma_{CO} + \gamma_{CO2} + \gamma_{CH4} - x$	(8)
Hydrogen Balance:	$f4 = 0 = 2\gamma_{H2} + 2\gamma_{H2O} + 4\gamma_{CH4} - y - 2a - 2b$	(9)
Oxygen Balance:	$f5 = 0 = \gamma_{CO} + \gamma_{H2O} + 2\gamma_{CO2} - z - 2a - 2b - 2c$	(10)
Nitrogen Balance:	$f6 = 0 = 2\gamma_{N2} - 2w$	(11)

The temperature dependency of equilibrium constants for WGS and MSR was obtained by means of the van't Hoff equation:

$$K(T) = K(T_0) \exp[\Delta H_R^0/R\ (1/T_0 - 1/T)] \quad (12)$$

where K(T) and K(T_0) are the values of the equilibrium constant at the reference temperature T_0[K] and at a given temperature T[K], R[J/mol·K] is the value of the universal gas constant and ΔH_R^0 is the standard reaction enthalpy at 298.15 K. In more details, the standard reaction enthalpy at 298.15 K is −41.1 kJ/mol in the case of the WGS reaction, which is moderately exothermic, and equal to 206.1 kJ/mol in the case of the endothermic reaction of methane steam reforming [40].

In order to obtain the values of γ_{N2}, γ_{H2O}, γ_{H2}, γ_{CO}, γ_{CO2} and γ_{CH4}, the six equations (Eqs. 6-11) were solved simultaneously by using the Standard Solver function available in the Microsoft Excel spreadsheet package on a conventional MS-Windows PC. The Solver uses the GRG Nonlinear Solving algorithm, which is one of the most robust programming methods to solve nonlinear algebraic problems [41].

2.3 Model validation

The model was validated by comparing its outputs, in terms of gas yields, with the experimental data by Qin et al. [16]. The comparison of results is reported in Table 2. In detail, the experimental yields in Table 2 are related to the test number wH3, wRl, wH1, wT5 [16], where approximately 12.8, 10.7, 12.8 and 12.8 g/min of wood (beech sawdust) were, respectively, fed to a lab-scale entrained flow gasifier by means of a cold feeder air flow rate of 10 Nl/min and then gasified at 1400 °C (with the exception of the test wT5 performed at 1000 ° C) by using only air (wT5) or air and steam mixtures (wH3, wRl, wH1) as gasifying agents. In particular, an excess air factor (λ) equal to 0.3 was adopted in all the above-mentioned tests, whereas the steam/carbon ratio

(mol/mol) was 0 in test wH3, 0.37 in tests wR1 e wT5 and 0.75 in test wH1. It is worth noting that the excess air factor (λ) adopted by Qui et al. (2012) [16], which indicates the ratio between the air supply and the air that is theoretically required for a complete feedstock combustion, does not include the air flow fed to the gasifier through the biomass feeding system. On the basis of these information, the equivalence ratio (ER) and the steam-to-biomass ratio on a dry ash free basis (SBR), to be used inputs in the model, were calculated as shown in Table 2. The quality of fit between experimental and simulated data was evaluated in terms of root mean square error (RMSE) as follows:

$$RMSE = \sqrt{\frac{\sum_{i=1}^{N}[(Experiment)_i - (Model)_i]^2}{N}} \quad (13)$$

where N is the number of data points for each set of data or gasification test. In detail, RMSE is a negatively oriented index score, which means lower values are better. It can range from 0 to ∞ and is expressed in the units of measurements of the variable of interest. In addition, RMSE is a quadratic index score, which gives a relatively high weight to large errors. This means that the RMSE is mostly useful when large errors are particularly undesirable. Results show that the model predictions provide a reasonable first approximation of the experimental data, particularly when the gasification process is performed at higher temperatures. This suggests that the adopted equilibrium model can be reliably used in the preliminary analysis and optimization of gasification processes performed in high temperature entrained flow reactor.

3 Results and discussion

The equilibrium model was used to investigate the effect of torrefaction pretreatment and the key gasification operating conditions - including the equivalence ratio (ER), the steam to biomass

312 ratio on a dry ash free basis (SBR) and the process temperature - on the quality of the product gas
313 arising from gasification of tomato peel residues with the steam and oxygen.

314 Fig. 1 shows the composition of the product gas obtained from the gasification of raw and
315 torrefied tomato peels (TPs) at 1300 °C by fixing the equivalence ratio (ER) at 0.4 while varying
316 SBR from 0.2 to 1.5 on a dry ash free basis, which are typical operating conditions for biomass
317 gasification in entrained flow reactors [10]. In detail, torrefied tomato peels, which had been
318 subjected to light (TP-200), medium (TP-240) and severe (TP-285) thermal treatment [24], were
319 selected to investigate the effect of torrefaction pretreatment severity. Model predictions show that
320 the gasification of torrefied feedstocks results in a product gas with a slightly higher concentration
321 of hydrogen (H_2) and carbon monoxide (CO) and a lower concentration of carbon dioxide (CO_2)
322 than the untreated biomass within the whole investigated steam-to-biomass range. In particular, the
323 higher the torrefaction temperature, the greater the concentration of H_2 and CO in the product gas
324 and the lower the CO_2 concentration. This findings can be explained by the lower values of O/C and
325 H/C atomic ratios of the biomass torrefied at higher temperature with respect to the raw feedstock
326 (see the Van Krevelen diagram in Fig. 4d), which favor the formation of CO and H_2 with respect to
327 H_2O and CO_2 [24]. Again, in accordance with the le Chatelier principle, it is found that higher SBR
328 ratios favor the conversion of CO to CO_2 and H_2 through the water gas shift reaction (Eq. 2)
329 whereas as regard CH_4, model predictions (not presented here) highlight that its volume fraction is
330 rather low when the gasification is performed at 1300 °C and ER = 0.4, resulting, in particular,
331 lower than 10 ppm in the case of both raw and torrefied TPs.

332 It is well known that the quality of the product gas mostly depend on the relative ratios
333 between its main components (i.e., CO, H_2, CO_2) rather than on their absolute volume fractions;
334 these ratios, in fact, determine not only its actual heating value (LHV) but also the complexity of
335 downstream processing required for its cleaning and upgrading and its final application [4]. The
336 H_2/CO and CO_2/CO ratios as well as the so called stoichiometric module $M = (H_2-CO_2)/(CO+CO_2)$
337 are commonly taken in the process industry as a measure of the eligibility of the product gas for

synthesis; specifically, the ideal H_2/CO ratio of the incoming syngas for Fischer-Tropsch (FT) synthesis is 2 whereas the required (H_2–CO_2)/(CO+CO_2) ratio for methanol production is 2.1. Therefore, in addition to the volume fractions of the main chemical species, the trends in such quality metrics were also investigated in order to determine operating conditions beneficial for obtaining a product gas suitable for synthesis rather than heat and power production. In more details, a comparison between the values of the H_2/CO, the CO_2/CO and the (H_2-CO_2)/(CO+CO_2) ratios arising from the gasification of both raw and torrefied tomato peels was performed for the different investigated operating conditions and the results are shown in Fig. 2 for the specific case of 1300 °C gasification temperature and 0.4 equivalence ratio. Model predictions highlight that the product gas obtained from the gasification of torrefied tomato peels is characterized by lower values of the H_2/CO ratio compared to that obtained by using raw tomato peels as feedstock, to an extent that increases with the increasing of torrefaction severity (Fig. 2a). Results also show that the increase in the torrefaction temperature promotes the decrease in the CO_2/CO ratio of the product gas (Fig. 2b) with the result that the stoichiometric number (M) and the lower heating value (LHV, dry basis) slightly rise after torrefaction treatment of the raw feedstock (Fig. 2c-d). This increase is even more significant at higher torrefaction temperature.

In this work, tomato peels subjected to a more severe torrefaction pretreatment (TP-285) were taken as the reference material in order to investigate the influence of the key gasification operating conditions, i.e. the equivalence ratio (ER), the steam to biomass ratio (SBR) and the process temperature, on the quality of the product gas arising from the gasification with steam and oxygen.

In particular, the volume fractions of the main components (i.e., CO, H_2, CH_4, CO_2) of the product gas, which is obtained by simulating the gasification of TP-285 at ER = 0.4 while changing SBR from 0.2 to 1.5 and the gasification temperature from 1000 °C to 1400 °C, are shown in Fig. 3. Data highlight that the product gas composition is very sensitive to both the variations of steam fuel ratio and temperature. In detail, it is found that higher SBR ratios favor the conversion of CO to

364 CO_2 and H_2 through the water gas shift reaction (Eq. 4) and provide favorable conditions for the
365 steam reforming of methane (Eq. 5) within the whole investigated temperature range. Again, it
366 results that the volume fraction of CO_2, H_2 and CH_4 decreases with the temperature, while the CO
367 concentration increases. This is in accordance with the Le Chatelier's principle that states that high
368 temperatures favor the reactants in exothermic reactions, such as the water-gas shift reaction ($\Delta H_R°$
369 = -41 kJ/mol), and products in the endothermic reactions, such as the steam reforming of methane
370 ($\Delta H_R°$ = 206 kJ/mol).
371 Fig. 4 shows the effect of the addition of different amounts of oxygen to the steam
372 gasification of TP-285 at 1300 °C; in particular, in this work, the equivalence ratio (ER) was
373 increased from 0 to 0.4 with a step of 0.1 while varying SBR in the range 0.2-1.5 on a dry ash free
374 basis. Model predictions suggest that the more the oxygen is added to the steam as a gasifying agent
375 the less the product gas composition is sensitive to the SBF variation. For example, it results that
376 the volume fraction of H_2 increases from 3 % to 58 % when SBF raises from 0.2 to 1.5 at ER = 0
377 whereas it just goes from 33% to 39 % when SBF changes from 0.2 to 1.5 at ER = 0.4 (Fig.4a). As
378 expected, it is found that the increase of the equivalence ratio leads to an over-oxidization or partial
379 combustion of the product gas to produce CO_2 (Fig. 4d) and H_2O (not shown here). Furthermore,
380 the equilibrium simulations show that the volume fraction of CH_4 in the product gas decreases
381 greatly with increasing the equivalence ratio from 0 to 0.4; in particular, its concentration turns out
382 to be almost equal to zero over the whole investigated SBR range when the value of the equivalence
383 ratio is equal or higher than 0.2 (Fig. 4b). As regards the volume fraction of H_2, data shown in
384 greater detail in Fig.5 demonstrate that it only starts to drop after reaching a peak value at ER = 0.2
385 when SBR is lower than 0.4 (Fig. 5a) whereas it steadily decreases with ER when SBR is in the
386 range of 0.4-1.5 (Fig. 5b). In contrast with what is typically observed in other studies modeling
387 gasification processes by means of equilibrium calculations [42, 43], the volume fraction of CO is
388 found to grow with the increase in the equivalence ratio. Anyway, this result is consistent with what

389 was observed by Babu and Sheth (2005) [44], who also studied the effect of oxygen enrichment and
390 steam-to-air ratio on the syngas composition by means of an equilibrium model.
391 Fig. 6, finally, shows the effect of the gasification temperature (Fig.6a,c,e) and the
392 equivalence ratio (Fig.6b,d,f) on the H_2/CO ratio, the stoichiometric module M and the lower
393 heating value of the product gas arising from the gasification of TP-285 with steam and oxygen.
394 Model predictions highlight that the decrease of the equivalence ratio (ER) results in a
395 product gas more suitable for energy application: in fact, the lower ER, the higher the LHV over the
396 investigated SBR range (Fig. 6e). Instead, as regards the use of the product gas for synthesis, it is
397 found that similar benefits are only get when the steam to biomass ratio is in the range of 0.7-1.5
398 (Fig6a,c). In fact, data shown in greater detail in Fig 5c-d display that for values of SBR lower than
399 0.7 a maximum value exists for both the H_2/CO ratio and the stoichiometric module at ER equal to
400 approximatively 0.1-0.2. Conversely, modeling results point out that lower gasification
401 temperatures promote not only a decrease in the product gas calorific value (Fig. 6f), but also make
402 it less suitable for synthesis applications as evidenced by the decrease in both the H_2/CO (Fig.6b)
403 and the (H_2-CO_2)/(CO+CO_2) ratios (Fig. 6d).
404
405 **3. Conclusions**
406 The simulation of oxygen-steam gasification of low value agro-industrial residues in a high
407 temperature entrained flow gasifier was performed in this work by using an equilibrium model.
408 Predictions on the composition and the calorific value of the producer gas arising from the
409 gasification of both raw and torrefied tomato peels were achieved by inserting in the model the
410 ultimate analysis data of the raw and torrefied solids resulting from fluidized bed torrefaction tests
411 performed in a previous work by the present authors. Four main variables, i.e., gasification
412 temperature, steam-to-biomass ratio, fuel-oxygen equivalence ratio and temperature of the
413 torrefaction pretreatment, were identified as inputs to the mathematical model. With respect to
414 them, a global sensitivity analysis was performed to assess the impact of both torrefaction

pretreatment and gasification operating conditions on the product gas quality in terms of lower heating value and typical composition metrics commonly taken in the process industry as a measure of the eligibility of the product gas for synthesis (i.e., H_2/CO ratio, stoichiometric module, etc.). An overall conclusion drawn from this analysis is that the torrefaction pretreatment provides only a marginal improvement in product gas quality despite the significant benefits it determine in biomass feeding, grinding, storage and feeding. In the present research work, however, only tomato peels were considered as a feedstock. Therefore, a further study is welcome on the effects of different types of non-woody biomass. Equilibrium simulations made available in the present study can be useful for a better understanding of the controlling variables that rule gasification processes in addition to act as a point of reference for more complex simulations of the high temperature entrained flow gasification of biomass with oxygen-steam mixtures.

References

[1] Bridgwater AV. The technical and economic feasibility of biomass gasification for power generation. Fuel 1995;74:631-653.

[2] Barba D, Capocelli M, Cornacchia G, Matera DA. Theoretical and experimental procedure for scaling-up RDF gasifiers: The Gibbs Gradient Method. Fuel 2016;179:60-70.

[3] Ruoppolo G, Miccio F, Brachi P, Picarelli A, Chirone R. Fluidized Bed Gasification of Biomass and Biomass/Coal Pellets in Oxygen and Steam Atmosphere. Chem Eng Trans 2013;32:595-600.

[4] Brachi P, Chirone R, Miccio F, Miccio M, Picarelli A, Ruoppolo G. Fluidized bed co-gasification of biomass and polymeric wastes for a flexible end-use of the syngas: Focus on bio-methanol. Fuel 2014;128:88-98.

[5] Basu, P. Biomass gasification, pyrolysis and torrefaction: practical design and theory. 2nd ed. London, UK: Academic press; 2013.

439 [6] Morrin S, Lettieri P, Chapman C, Mazzei L. Two stage fluid bed-plasma gasification process for
440 solid waste valorization: Technical review and preliminary thermodynamic modelling of sulphur
441 emissions. Waste Manage 2012;32:676-684.
442 [7] Kumar S, Shukla SK. A Review on Recent Gasification Methods for Biomethane Gas
443 Production. Int J Energy Eng 2016;6:32-43.
444 [8] Lv P, Yuan Z, Ma L, Wu C, Chen Y, Zhu J. Hydrogen-rich gas production from biomass air and
445 oxygen/steam gasification in a downdraft gasifier. Renew Energ 2007;32:2173-2185.
446 [9] Van Huynh C, Kong SC. Combustion and NOx emissions of biomass-derived syngas under
447 various gasification conditions utilizing oxygen-enriched-air and steam. Fuel 2013;107:455-464.
448 [10] Surjosatyo A, Vidian F, Nugroho YS. Experimental Gasification of Biomass in an Updraft
449 Gasifier with External Recirculation of Pyrolysis Gases. J Combust 2014;2014:1-6.
450 [11] Zhou J, Chen Q, Zhao H, Cao X, Mei Q, Luo Z, Cen K. Biomass-oxygen gasification in a
451 high-temperature entrained-flow gasifier. Biotechnol Adv 2009;27: 606- 611.
452 [12] Qin K, Lin W, Jensen PA, Jensen AD. High-temperature entrained flow gasification of
453 biomass. Fuel 2012;93:589-600.
454 [13] Bergman PCA, Boersma AR, Kiel JHA, Prins MJ, Ptasinski K.J, Janssen FJJG. Torrefaction
455 for entrained-flow gasification of biomass. ECN Report No.: ECN-C-05-067(2005).
456 https://www.ecn.nl/docs/library/report/2005/c05067.pdf. [accessed 06 December 2017].
457 [14] Senapati PK, Behera S. Experimental investigation on an entrained flow type biomass
458 gasification system using coconut coir dust as powdery biomass feedstock. Bioresour Technol
459 2012;117:99-106.
460 [15] Hernández JJ, Aranda G, Barba J, Mendoza JM. Effect of steam content in the air–steam flow
461 on biomass entrained flow gasification. Fuel Process Technol 2012;99:43-55.
462 [16] Qin K, Jensen PA, Lin W, Jensen AD. Biomass Gasification Behavior in an Entrained Flow
463 Reactor: Gas Product Distribution and Soot Formation. Energy Fuels 2012;26:5992-6002.

[17] Hernandez JJ, Almansa GA, Bula A. Gasification of biomass wastes in an entrained flow gasifier: effect of the particle size and the residence time. Fuel Process Technol 2010;9:681-692.

[18] Umeki k, Häggström G, Bach-Oller A, Kirtania K, Furusjö E. Reduction of tar and soot formation from entrained-flow gasification of woody biomass by alkali impregnation. Energy Fuels 2017;31:5104-5110.

[19] Briesemeister L, Kremling M, Fendt S, Spliethoff H. Air-Blown Entrained-Flow Gasification of Biomass: Influence of Operating Conditions on Tar Generation. Energy Fuels 2017;31:10924–10932.

[20] Xiao R, Chen X, Wang F, Yu G. Pyrolysis pretreatment of biomass for entrained-flow gasification. Appl Energy 2010;87:149-155.

[21] Weiland F, Nordwaeger M, Olofsson I, Wiinikka H, Nordin A. Entrained flow gasification of torrefied wood residues. Fuel Process Technol 2014;125:51-58.

[22] Ku X, Lin J, Yuan F. Influence of Torrefaction on Biomass Gasification Performance in a High-Temperature Entrained-Flow Reactor. Energy Fuels 2016;30:4053-4064.

[23] Brachi P, Miccio F, Ruoppolo G, Miccio M. Pressurized Steam Torrefaction of Biomass: Focus on Solid, Liquid, and Gas Phase Distributions. Ind Eng Chem Res,2017;56:12163–12173.

[24] Brachi P, Miccio F, Miccio M, Ruoppolo G. Torrefaction of Tomato Peel Residues in a Fluidized Bed of Inert Particles and a Fixed-Bed Reactor. Energy Fuels 2016;30:4858-4868.

[25] Rousset P, Petithuguenin T, Rodrigues T, Azevedo AC. The fluidization behavior of torrefied biomass in a cold model. Fuel 2012;102:256-263.

[26] Fisher EM, Dupont C, Darvell LI, Commandré JM, Saddawi A, Jones JM, Grateau M, Nocquet T, Salvador S. Combustion and gasification characteristics of chars from raw and torrefied biomass. Bioresour Technol 2012;119: 157-165.

[27] Brachi P, Riianova E, Miccio M, Miccio F, Ruoppolo G, Chirone R. Valorization of Sugar Beet Pulp via Torrefaction with a Focus on the Effect of the Preliminary Extraction of Pectins. Energy Fuels 2017;31:9595–9604.

490 [28] Brachi P, Miccio F, Miccio M, Ruoppolo G. Pseudo-component thermal decomposition
491 kinetics of tomato peels via isoconversional methods. Fuel Process Technol 2016;154:243-250.
492 [29] Martis MS. Validation of simulation based models: a theoretical outlook. Electron J Bus Res
493 Methods 2005;4:39-46.
494 [30] Żogała A. Critical analysis of underground coal gasification models. Part I: equilibrium models
495 - literary studies. J Sust Min 2014;13:22-28.
496 [31] Furusjö E, Jafri Y. Thermodynamic equilibrium analysis of entrained flow gasification of spent
497 pulping liquors. Biomass Conv Bioref 2016:1-13.
498 [32] Detournay M, Hemati M, Andreauz R. Biomass steam gasification in fluidized bed of inert or
499 catalytic particles: Comparison between experimental results and thermodynamic equilibrium
500 prediction. Powder Technol 2011;208:558-557.
501 [33] Jarungthammachote S, Dutta A. Thermodynamic equilibrium model and second law analysis
502 of a downdraft waste gasifier. Energy 2007;32:1600-1669.
503 [34] Altafini CR, Wander PR, Barreto RM. Prediction of the working parameters of a wood waste
504 gasifier through an equilibrium model. Energ Convers Manage 2003;44:2763-2777.
505 [35] Salaices E, Serrano B, de Lasa H. Biomass Catalytic Steam Gasification Thermodynamics
506 Analysis and Reaction Experiments in a CREC Riser Simulator. Ind Eng Chem Res 2010;49:6834-
507 6844.
508 [36] Puig-Arnavat M, Bruno JB, Coronas A. Modified Thermodynamic Equilibrium Model for
509 Biomass Gasification: A Study of the Influence of Operating Conditions. Energy Fuels
510 2012;26:1385−1394.
511 [37] Tassios DP. Applied chemical engineering thermodynamics. Berlin: Springer-Verlag; 1993.
512 [38] Vaezi M, Passandideh-Fard M, Moghiman M, Charmchi M. Modeling Biomass Gasification:
513 A New Approach to Utilize Renewable Sources of Energy. Proc ASME International Mechanical
514 Engineering Congress and Exposition, Boston, MA, Paper No. IMECE2008-68707, pp. 927-935.

515 [39] Mountourius A, Voutsas E, Tassios T. Solid waste plasma gasification: Equilibrium model
516 development and exergy analysis. Energ Convers Manage 2006;47:1723-1737.
517 [40] Bobrova L, Andreev D, Ivanov E, Mezentseva N, Simonov M, Makarshin L, Cribovskii A,
518 Sadykov V. Water-gas shift reaction over Ni/CeO_2 catalysts. Catalysts 2017;7:1-24.
519 [41] Lwin Y. Chemical equilibrium by Gibbs energy minimization on spreadsheets. Int J Eng Educ
520 2000;16:335-339.
521 [42] Echegaray M, Rodriguez R, Rosa Castro M. Equilibrium model of the gasification process of
522 agro industrial wastes for energy production. Int J Eng Sc Innov Tech 2014;3:6-17.
523 [43] Vaezi M, Passandideh-Fard M, Moghiman M, Charmchi M. Gasification of heavy fuel oils: a
524 thermochemical equilibrium approach. Fuel. 2011;90:878–885
525 [44] Babu BV, Sheth PN. Modelling & simulation of biomass gasifier: Effect of Oxygen
526 Enrichment and Steam-to-air Ratio. Proc International congress on renewable energy (ICORE-
527 2005), Pune, Paper No. 30, pp 194-204.

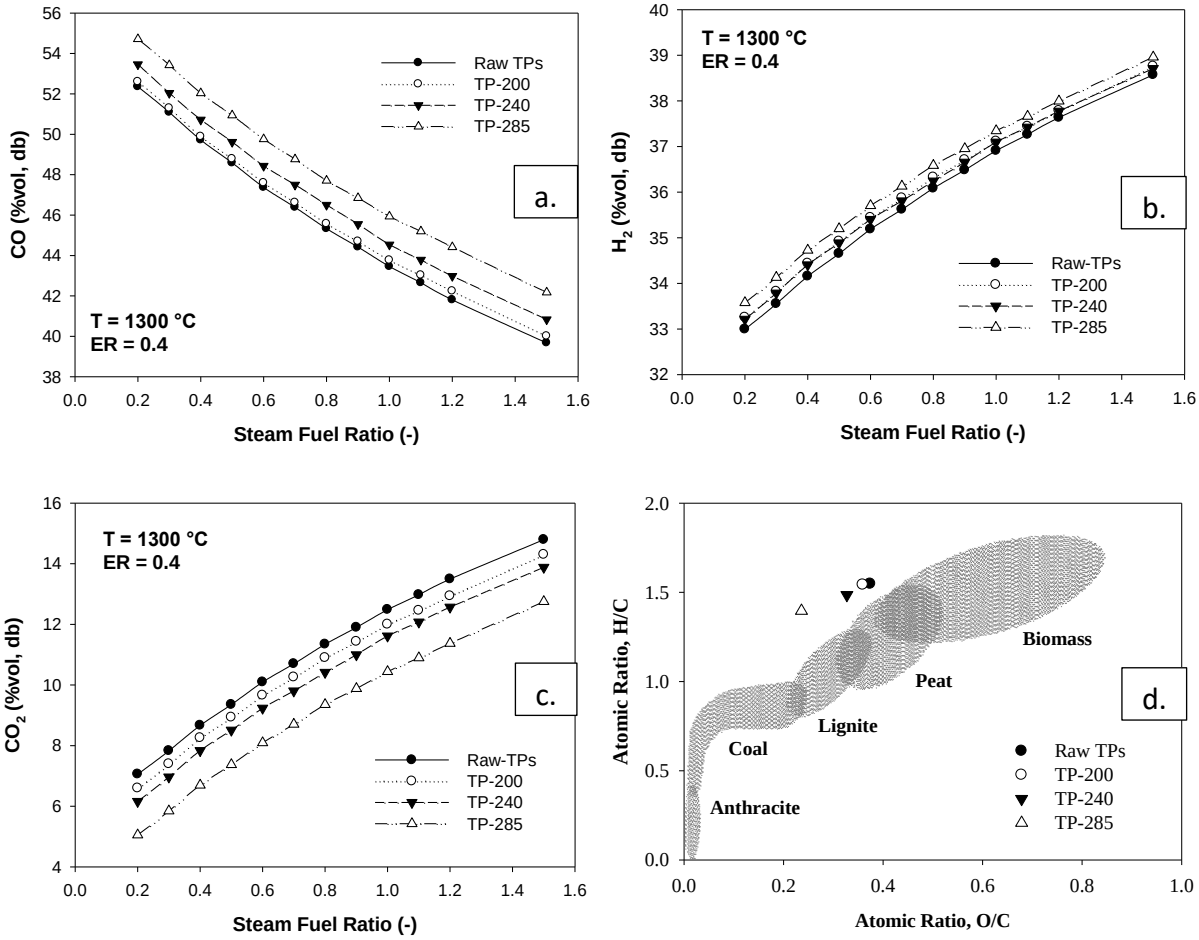

Fig. 1 Effect of the steam-fuel ratio and the feedstock torrefaction temperature on the product gas composition at 1300 °C and ER = 0.4 and Van Krevelen diagram of torrefied tomato peels obtained from fluidized bed torrefaction tests [15].

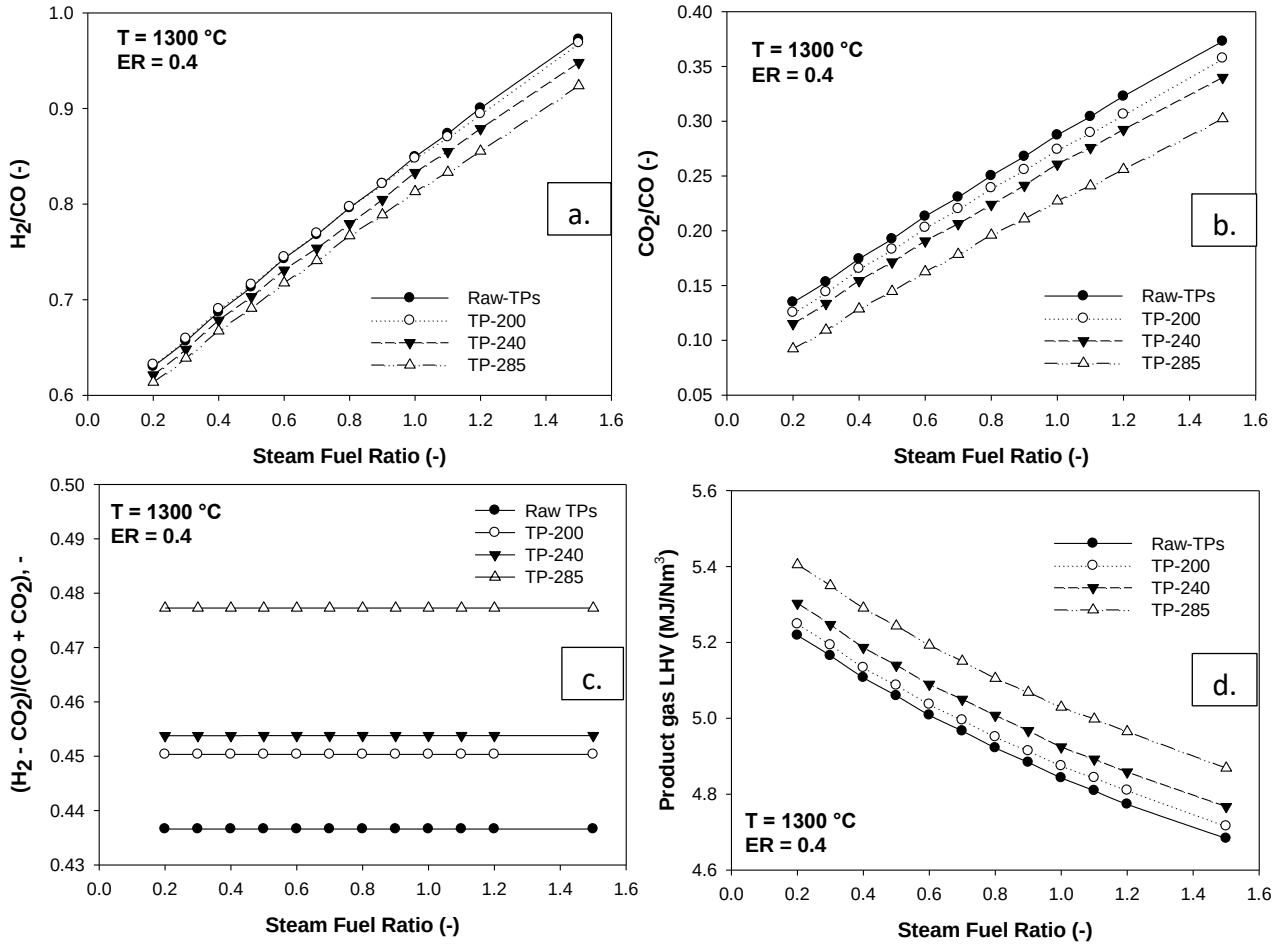

Fig. 2 Effect of the steam-fuel ratio and the feedstock torrefaction temperature on the composition and the lower heating value of the product gas arising from the gasification process performed at 1300 °C and ER = 0.4.

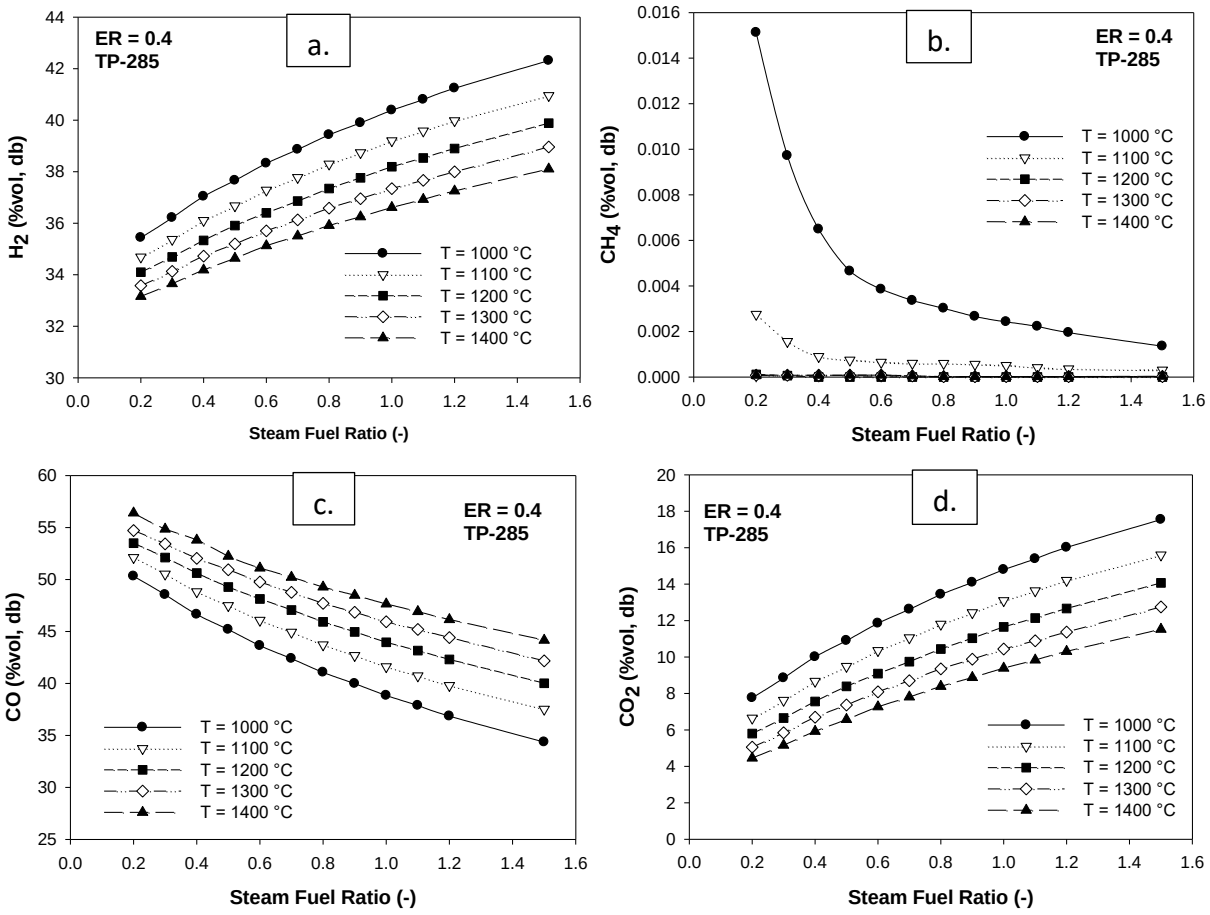

538

539

540 **Fig. 3** Effect of the gasification temperature and the steam-fuel ratio on the composition of the product
541 gas arising from the gasification of the TP-285 feedstock with ER = 0.4.

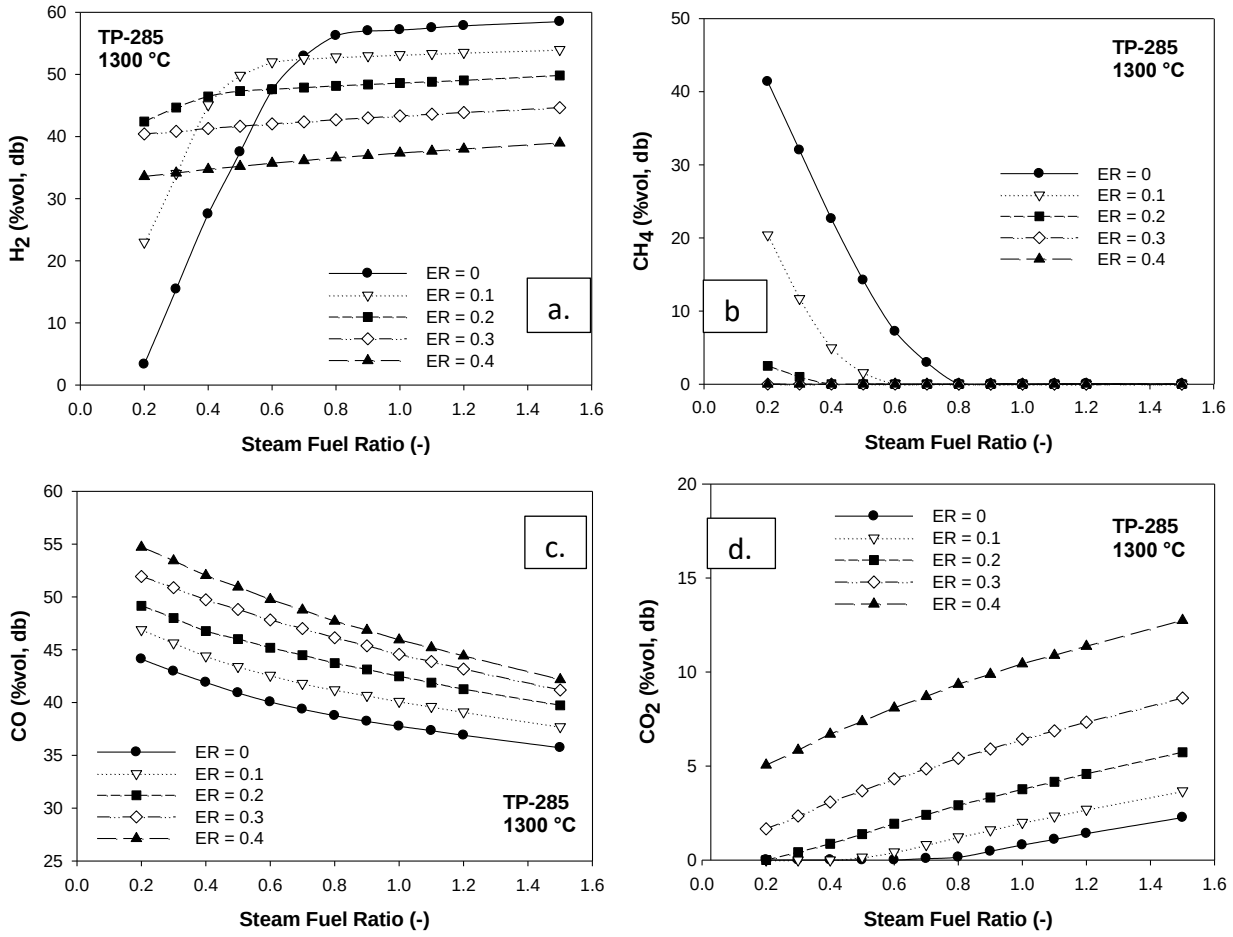

Fig. 4 Effect of the equivalence ratio (ER) and the steam-biomass ratio on the product gas composition arising from the gasification of the TP-285 feedstock at 1300 °C.

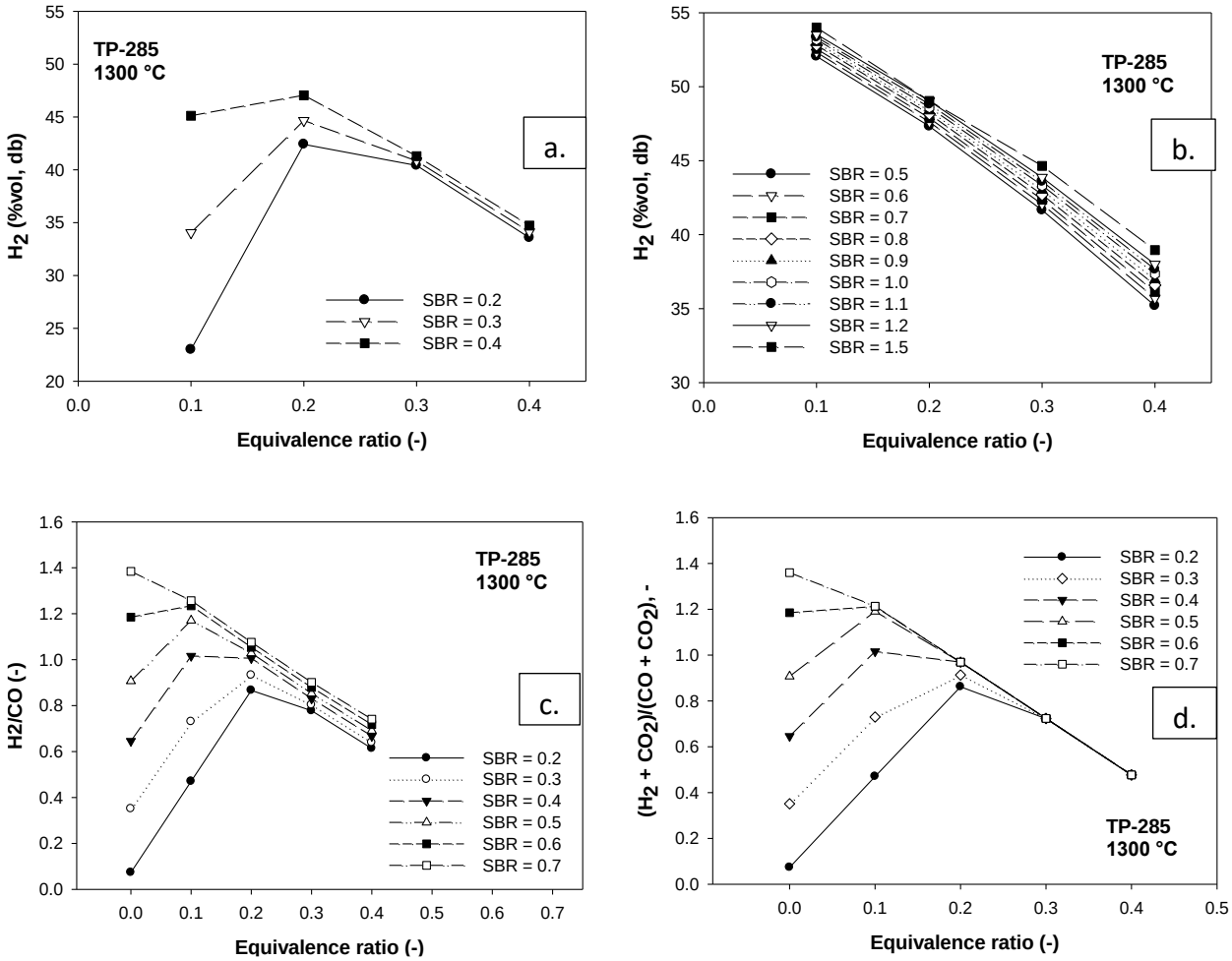

Fig. 5 Effect of the equivalence ratio and the steam-biomass ratio on the H_2 volume fraction in the product gas generated by the gasification of the TP-285 feedstock at 1300 °C.

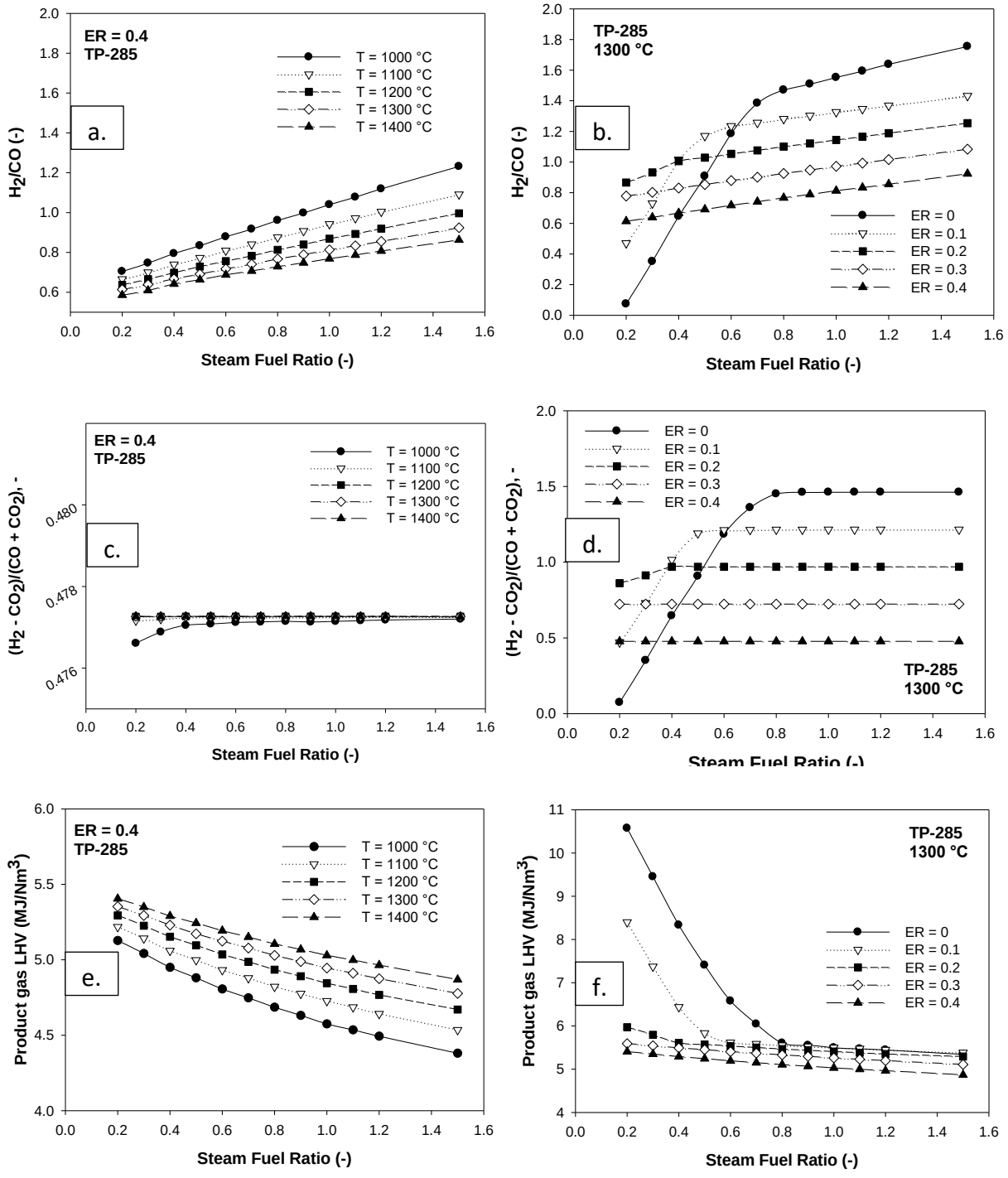

Fig. 6 Effect of equivalence ratio and gasification temperature on the composition and the lower heating value of the product gas arising from the gasification of the TP-285 feedstock by varying the steam-biomass ratio from 0.2 to 1.5.

Table 1. Elemental analysis, ash content and calorific value of the selected biomass feedstock [15].

Sample	**C (%wt., db)**	**H (%wt., db)**	**N (%wt., db)**	**O (%wt., db)**	**Ash (%wt., db)**	**LHV (MJ/kg, db)**
Raw TPs	58.38	7.72	1.49	30.60	1.81	24.14
TP-200	59.53	7.74	1.82	28.35	2.57	24.56
TP-240	61.65	7.72	1.52	26.53	2.58	25.25
TP-285	66.40	7.78	1.66	20.87	3.29	29.33

Table 2. Comparison of gasification results between equilibrium calculations and experimental data [16].

Feedstock	SBR	ER	T (°C)	TEST [12]	Gas yields	CO	CO_2	CH_4	H_2	RMS
						(Nm^3/ $kg_{wood,daf}$)				
Wood	0	0.47	1400	WH3	Experimental	0.67	0.19	< 0.01	0.42	0.11
					Model	0.82	0.19	< 0.01	0.31	
Wood	0.37	0.51	1400	WR1	Experimental	0.61	0.25	< 0.01	0.50	0.12
					Model	0.73	0.29	< 0.01	0.33	
Wood	0.75	0.47	1400	WH1	Experimental	0.55	0.32	< 0.01	0.56	0.13
					Model	0.71	0.31	< 0.01	0.42	
Wood	0.37	0.47	1000	WT5	Experimental	0.29	0.37	< 0.01	0.27	0.23
					Model	0.64	0.37	< 0.01	0.49	

* **Dry wood composition**: $CH_{3.05}O_{1.32}N_{0.05}$; **Moisture**: 9.04 %wt., a.r.; **Ash** = 0.67 %wt., db.